



**HAL**  
open science

# Semi-Implicit Homogeneous Euler Differentiator for a Second-Order System: Validation on Real Data

Loïc Michel, Malek Ghanes, Franck Plestan, Yannick Aoustin, Jean-Pierre Barbot

► **To cite this version:**

Loïc Michel, Malek Ghanes, Franck Plestan, Yannick Aoustin, Jean-Pierre Barbot. Semi-Implicit Homogeneous Euler Differentiator for a Second-Order System: Validation on Real Data. IEEE CDC 2021, Dec 2021, Austin (Texas), United States. hal-03414289v2

**HAL Id: hal-03414289**

**<https://hal.science/hal-03414289v2>**

Submitted on 4 Apr 2022

**HAL** is a multi-disciplinary open access archive for the deposit and dissemination of scientific research documents, whether they are published or not. The documents may come from teaching and research institutions in France or abroad, or from public or private research centers.

L'archive ouverte pluridisciplinaire **HAL**, est destinée au dépôt et à la diffusion de documents scientifiques de niveau recherche, publiés ou non, émanant des établissements d'enseignement et de recherche français ou étrangers, des laboratoires publics ou privés.

# Semi-Implicit Homogeneous Euler Differentiator for a Second-Order System: Validation on Real Data

Loïc MICHEL, Malek GHANES, Franck PLESTAN, Yannick AOUSTIN and Jean-Pierre BARBOT

**Abstract**—In this paper, a semi-implicit Euler approximation scheme is proposed for a second-order homogeneous differentiator. Compared to an explicit Euler approximation, it is well-known that implicit Euler approximation scheme offers better performances like reducing high frequency oscillations. However, the implicit Euler approximation scheme works well only when dealing with classical sliding mode differentiator. In order to keep advantages of implicit Euler approximation, when this approximation is applied in case of homogeneous differentiators, a semi-implicit Euler approximation is proposed for a second-order system. Validation on real data is conducted to highlight the well-founded of the proposed differentiation strategy.

**Index Terms**—Discretization, Homogeneous differentiator, Attractor, Projectors, Experimental Data.

## I. INTRODUCTION

This paper is dedicated to a real signal differentiation problem that is a crucial problem from a practical point-of-view; for example in robotics, a speed sensor is more expensive and fragile than an encoder sensor [1], [2]. Numerical differentiation is then preferred to design model based control. However, digital differentiation in the presence of Coulomb friction or noise can lead to instability or, at least, to high frequency phenomena of the closed loop system. This could be dramatic for example with a haptic control in a medical application.

Improving the operation of differentiation is complex and therefore attracts the interest of a lot of scientists and a comparison of some of them has been performed in [3]. The differentiation problem can be treated by two ways. The first way consists in using continuous-time differentiators [4] based on, for example, higher order sliding mode approaches and especially the well-known super-twisting algorithm [5]. The second way is closer to real systems that are driven by discretized algorithms, and deals with differentiators based on numerical Euler approximation. In the literature, two approaches of Euler approximation can be used.

The first one is a classical Euler explicit approximation approach, which has some drawbacks with respect to high frequency oscillations phenomena, see for example [3]. Note that, in [6], an explicit discrete differentiator including additional Taylor expansion corrective terms is proposed.

L. MICHEL, M. GHANES, F. PLESTAN and J.-P. BARBOT are with École Centrale de Nantes-LS2N, UMR 6004 CNRS, Nantes, France {loic.michel, malek.ghanes, franck.plestan}@ec-nantes.fr

Y. AOUSTIN is with Université de Nantes-LS2N, UMR 6004 CNRS, Nantes yannick.aoustin@univ-nantes.fr

J.-P. BARBOT is also with QUARTZ EA 7393, ENSEA, Cergy-Pontoise, France barbot@ensea.fr

Moreover, in [7], the accuracy of such explicit discrete differentiator is studied. The second one, introduced in [8], is based on Euler implicit approximation approach and allows reducing significantly the oscillation phenomena whatever the actuator gain is [9]. In addition, a comparison of performances among 25 classical and advanced differentiation structures has been performed [3], [10] and highlights the fact that implicit based methods are more efficient and robust to the noise than the corresponding explicit strategies.

Motivated by this ascertainment, this paper proposes a semi-implicit approximation, which is a combination between explicit and implicit techniques in order to be able to deal with homogeneous differentiators while keeping the benefits of Euler implicit approximation in the context of second order-system. The main contribution of the proposed differentiator is to combine explicit part with implicit one based on two *projectors* in order to reduce the effects of chattering phenomena as well as measurement noise and perturbations. To prove this claim, a theoretical study estimating the oscillation amplitude is firstly given in the context of explicit discretization in one dimensional case. To highlight the merit of the proposed strategy, experiments are conducted within an electrical RC circuit.

This paper is outlined as follows. Section II describes the background of the homogeneous differentiation approach. Section III presents the main contribution and describes the semi-implicit homogeneous approach including a single projector, whereas the extension with two projectors is presented in Section IV. Section V describes a modification of the projectors to improve the robustness with respect to the noise. Both differentiation approaches are applied to experimental data in Section VI in which their benefits are discussed. Section VII concludes the paper and suggests some future works.

## II. BACKGROUND ON HOMOGENEOUS DIFFERENTIATION

### A. Basic analysis on the explicit Euler discretization

To introduce the homogeneous approach, consider the following continuous time system

$$\dot{x} = a \quad (1)$$

where  $a$  is a constant perturbation. A continuous time estimator for (1) reads as (with  $b > 0$ )

$$\dot{\hat{x}} = b[x - \hat{x}]^\alpha \quad (2)$$

where the notation  $[\bullet]^\alpha = |\bullet|^\alpha \text{sgn}(\bullet)$  is adopted all along the paper. So, the dynamics of the estimation error  $e = x - \hat{x}$

read as

$$\dot{e} = a - b[e]^\alpha \quad (3)$$

Setting  $\alpha \in (0, 1)$ , and supposing that  $b$  is sufficiently large versus  $a$ , i.e.  $b \gg |a|$ ,  $e$  converges to  $e_{eq} = \lceil \frac{a}{b} \rceil^{\frac{1}{\alpha}}$  in a finite time  $t_f > 0$ . The explicit Euler discretization of (3) gives

$$e^+ = e + h(a - b[e]^\alpha), \quad (4)$$

where the notation  $\bullet^+ = \bullet(k+1)$  is adopted in the discrete-time framework along the paper. For ease of reading, notation "e" is kept in the term of the right part of (4), but the term has also to be considered in the discrete-time framework; the equilibrium point of (4) being exactly the same than (3) i.e.  $e_{eq} = \lceil \frac{a}{b} \rceil^{\frac{1}{\alpha}}$ . Remark that if  $\alpha = 0$ , then  $e_{eq} \rightarrow 0$  since  $b > a$ . In the sequel, two cases  $\alpha \in (0, 1)$  and  $\alpha > 1$  are considered. The particular case  $\alpha = 1$  will be discussed at the end of this section.

### CASE 1: $0 < \alpha < 1$ .

It is well-known that  $e$  oscillates in the case of (4); considering the change of coordinate  $e = z + e_{eq}$  yields to

$$z^+ = z + h(a - b[z + e_{eq}]^\alpha). \quad (5)$$

A graph of  $z^+$  versus  $z$  for  $ha = 10^{-3}$ ,  $hb = 1.7783$  and  $\alpha = 0.75$  is displayed Fig. 1.

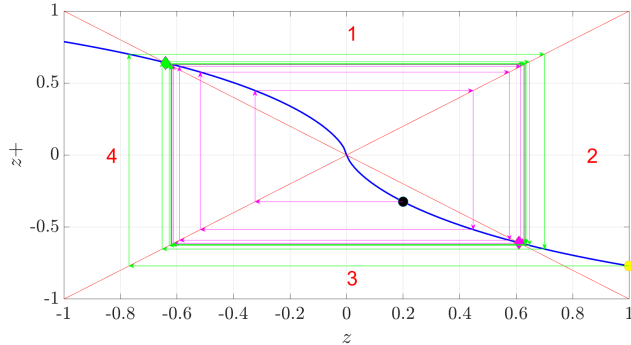


Fig. 1.  $z^+$  versus  $z$  (blue line) for  $\alpha = 0.75$ .

From Fig. 1, quarters 1 and 3 appear to be unstable, whereas the quarters 2 and 4 are stable: as a consequence, contrarily to (3), the equilibrium point  $e_{eq}$  is unstable for (4). Fig. 1 allows to define the domain  $\Omega$  such that

$$\Omega = \{z, z^+ / z_{os1} \leq z \leq z_{os2}, z_{os1} \leq z^+ \leq z_{os2}\}$$

where  $z_{os1}$  is the value of the abscissa of the point marked with a green diamond, and  $z_{os2}$  is the value of the abscissa of the point marked with a magenta diamond. Starting for example from the initial value denoted  $z_0 = 0.2$  (marked with a black bullet), the system (5) converges to a limit cycle, whose behaviour oscillates between  $z_{os1}$  and  $z_{os2}$  such that

$$z_{os2} = -z_{os1} \approx 0.6$$

as shown in Fig. 2. Now, with respect to Fig. 1, in order to evaluate the magnitude of the oscillation, it is necessary to evaluate a majorant of the non-zero coordinates of the

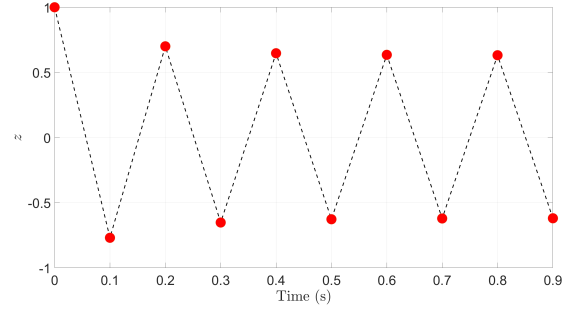


Fig. 2.  $z$  versus  $t$  (sec) for  $z(0) = 1$ .

intersection point, denoted  $z_{int}$ , between  $z^+$ -function (blue line - Fig. 1) and red lines of Fig. 1. The intersection points are defined such that

$$-z_{int} = z_{int} + h(a - b[z_{int} + e_{eq}]^\alpha)$$

which gives

$$2z_{int} = hb[z_{int} + e_{eq}]^\alpha - ha. \quad (6)$$

Replacing  $e_{eq}$  by  $\lceil \frac{a}{b} \rceil^{\frac{1}{\alpha}}$ , equation (6) becomes

$$2z_{int} = hb[z_{int} + \lceil \frac{a}{b} \rceil^{\frac{1}{\alpha}}]^\alpha - ha$$

or

$$2z_{int} = h(\lceil b^{\frac{1}{\alpha}} z_{int} + \lceil a \rceil^{\frac{1}{\alpha}} \rceil^\alpha - a). \quad (7)$$

Assuming that there exists  $w$  such that  $z_{int} = \lceil w \rceil^{\frac{1}{\alpha}}$ , equation (7) gives (8) and allows determining a majorant of  $z_{int}$  depending on the following sign conditions:

$$2z_{int} = h(\lceil \lceil bw \rceil^{\frac{1}{\alpha}} + \lceil a \rceil^{\frac{1}{\alpha}} \rceil^\alpha - a) \quad (8)$$

1) if  $\text{sgn}(\lceil bw \rceil^{\frac{1}{\alpha}} + \lceil a \rceil^{\frac{1}{\alpha}}) \text{sgn}(a) = 1$ , then two cases occur

a) if  $\lceil \lceil bw \rceil^{\frac{1}{\alpha}} + \lceil a \rceil^{\frac{1}{\alpha}} \rceil^\alpha > |a|$  then, from Jensen inequality dedicated to the convex functions [11], one has

$$\lceil \lceil bw \rceil^{\frac{1}{\alpha}} + \lceil a \rceil^{\frac{1}{\alpha}} \rceil^\alpha \leq |bw| + |a|$$

and from (8), one gets

$$|2z_{int}| \leq h|bw| + |a| - |a| = h|bw| = hb|z_{int}|^\alpha$$

that gives the inequality

$$|z_{int}| = \left(\frac{hb}{2}\right)^{\frac{1}{1-\alpha}}.$$

b) if  $\lceil (bw)^{\frac{1}{\alpha}} + a^{\frac{1}{\alpha}} \rceil^\alpha \leq |a|$ , it comes from (8)

$$|2z_{int}| \leq |ha|$$

then, for  $\text{sgn}(\lceil bw \rceil^{\frac{1}{\alpha}} + \lceil a \rceil^{\frac{1}{\alpha}}) \text{sgn}(a) = 1$ , one has

$$|z_{int}| \leq \max \left\{ \left(\frac{hb}{2}\right)^{\frac{1}{1-\alpha}}, \frac{h|a|}{2} \right\}. \quad (9)$$

2) if  $\text{sgn}(\lceil bw \rceil^{\frac{1}{\alpha}} + \lceil a \rceil^{\frac{1}{\alpha}}) \text{sgn}(a) = -1$ , it implies  $|bw|^{\frac{1}{\alpha}} > |a|^{\frac{1}{\alpha}}$ . As a consequence,  $|\lceil bw \rceil^{\frac{1}{\alpha}} + \lceil a \rceil^{\frac{1}{\alpha}}| < |bw|^{\frac{1}{\alpha}}$  and  $|ha| < h|bw|$ . Then, equation (7) gives

$$\begin{aligned} |2z_{int}| < h|bw| + h|bw| &\Rightarrow |z_{int}| < hb|z_{int}|^{\alpha} \\ &\Rightarrow |z_{int}| < (hb)^{\frac{1}{1-\alpha}}. \end{aligned}$$

From (9) and the previous inequation, the worth case is

$$|z_{int}| < (hb)^{\frac{1}{1-\alpha}}. \quad (10)$$

**CASE 2:**  $\alpha > 1$ .

Figure 3 displays  $z^+$  versus  $z$  for  $ha = 10^{-3}$ ,  $hb = 1.7783$  and  $\alpha = 2$ . It can be seen that the equilibrium point  $e_{eq}$  is stable.

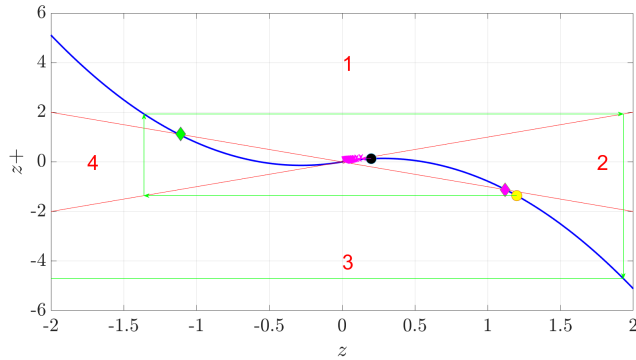


Fig. 3.  $z^+$  versus  $z$  (blue line) for  $\alpha = 2$ .

Moreover, in Fig. 3, green and magenta diamonds highlight the points allowing to define the attractivity domain of  $e_{eq}$ . Starting with an initial condition far from the equilibrium point, *i.e.* over the diamonds w.r.t. the origin of the  $(z, z^+)$ -plane, the explicit Euler discretization generates an unstable solution.

**Remark 1:** For the specific case  $\alpha = 1$ , the curve is a line crossing the origin and either the line is included inside the quarters 1 or 3, and therefore (4) is unstable, or the line is included inside the quarters 2 and 4, and consequently (4) is globally stable. Moreover in (9) and (10), it not possible to consider the case  $\alpha = 1$  because the limit goes to  $\infty$ . ■

*B. Some recalls on two dimensional case*

**Continuous-time system.** Let  $p(t)$  be a bounded perturbation, which is considered unknown. The system under study consists of a double integrator defined as

$$\begin{cases} \dot{x}_1 = x_2 \\ \dot{x}_2 = p(t) \\ y = x_1 \end{cases} \quad (11)$$

where  $x(t) \in \mathbb{R}^2$  is the state of the system, and  $y \in \mathbb{R}$  is the output of the system.

**Assumption 1:** There exists  $p_M > 0$  such that  $|p(t)| < p_M$  for all  $t > 0$ . ■

**Homogeneous continuous-time differentiator.**

Given Assumption 1, from [12], [13], a continuous-time homogeneous differentiator can be designed as follows

$$\begin{cases} \dot{z}_1 = z_2 + \lambda_1 \mu \lceil \epsilon_1 \rceil^{\alpha} \\ \dot{z}_2 = \lambda_2 \mu^2 \lceil \epsilon_1 \rceil^{2\alpha-1} \end{cases} \quad (12)$$

where  $\epsilon_1 = x_1 - z_1$ . The gains  $\lambda_i > 0$ ,  $i = \{1, 2\}$  and the parameter  $\mu$  (sufficiently large to cancel the effect of  $p(t)$ ) are tuned such that  $\epsilon_1$  and  $\epsilon_2 = z_2 - x_2$  converge towards zero. Then, the system (12) allows to get an estimation of  $\dot{x}_1$  thanks to  $z_2$ .

**Implicit Euler discrete-time system.** Given Assumptions 1-2 on  $p(t)$  and  $h$ , the implicit Euler discretization of continuous-time system (11) reads as

$$\begin{cases} x_1^+ = x_1 + h x_2^+ = x_1 + h(x_2 + h p^+) \\ x_2^+ = x_2 + h p^+ \end{cases} \quad (13)$$

**Objective.** The objective is now to propose an Euler discretization of the continuous-time homogeneous second-order differentiator (12). Two possibilities can be offered:

- **Explicit homogeneous Euler differentiator** This solution consists in proposing an explicit Euler approximation of the differentiator (12)

$$\begin{cases} \hat{x}_1^+ = \hat{x}_1 + h(\hat{x}_2 + \lambda_1 \lceil e_1 \rceil^{\alpha}) \\ \hat{x}_2^+ = \hat{x}_2 + h(\lambda_2 \lceil e_1 \rceil^{2\alpha-1}) \end{cases} \quad (14)$$

where  $e_1 = x_1 - \hat{x}_1$ .

However, this solution based on (14) is not attractive since it suffers of chattering phenomenon.

- **Implicit homogeneous Euler differentiator** This solution reading as

$$\begin{cases} \hat{x}_1^+ = \hat{x}_1 + h(\hat{x}_2^+ + \lambda_1 \lceil e_1^+ \rceil^{\alpha}) \\ \hat{x}_2^+ = \hat{x}_2 + h(\lambda_2 \lceil e_1^+ \rceil^{2\alpha-1}) \end{cases} \quad (15)$$

allows to propose an implicit Euler approximation [8] of (12) in the case of  $\alpha = 0.5$  (Levant differentiator).

It can be noticed that, from (15), the observation error equation reads

$$e_1^+ = e_1 + h(e_2^+ + \lambda_1 \lceil e_1^+ \rceil^{\alpha}). \quad (16)$$

Remark that it is impossible to solve (16) under the constraint  $e_1^+ = 0$  for  $\alpha \neq 0$  due to the presence of  $\lceil e_1^+ \rceil^{\alpha}$  associated to the correction term. Consequently, the implicit homogeneous Euler second-order differentiator (15) does not work. That is the reason why, in the next section, a semi-implicit homogeneous Euler second-order differentiator is proposed, and its accuracy is evaluated considering experimental data.

### III. SEMI-IMPLICIT HOMOGENEOUS EULER DIFFERENTIATOR WITH ONE PROJECTOR

A semi-implicit Euler discretization of the homogeneous differentiator (12) with a single projector (SIHD-1) is proposed and reads as

$$\begin{cases} \hat{x}_1^+ = \hat{x}_1 + h(\hat{x}_2^+ + \lambda_1 \mu |e_1|^\alpha \mathcal{N}_1) \\ \hat{x}_2^+ = \hat{x}_2 + E_1^+ h(\lambda_2 \mu^2 |e_1|^{2\alpha-1} \mathcal{N}_1) \end{cases} \quad (17)$$

where

$$\mathcal{N}_1 := \begin{cases} |e_1|^{1-\alpha} < \lambda_1 \mu h \quad (e_1^+ = 0) \rightarrow \mathcal{N}_1 = \frac{|e_1|^{1-\alpha}}{\lambda_1 h \mu} \\ |e_1|^{1-\alpha} \geq \lambda_1 \mu h \quad (e_1^+ \neq 0) \rightarrow \mathcal{N}_1 = \text{sgn}(e_1) \end{cases} \quad (18)$$

is the projector that replaces the function  $\text{sgn}(e_1^+)$  in (15); see [8] for detailed explanations.

**Remark 2:** As it is not possible to solve (16) because of the term  $|e_1^+|^\alpha \text{sgn}(e_1^+)$ , this latter is replaced in the proposed method by  $|e_1|^\alpha \mathcal{N}_1$ , where  $\mathcal{N}_1$  formally replaces  $\text{sgn}(e_1^+)$ . ■

Moreover,  $E_1^+$  is defined as

$$E_1^+ = \begin{cases} 1 & \text{if } e_1 \in SD \\ 0 & \text{if } e_1 \notin SD \end{cases} \quad (19)$$

with  $SD$  defined as

$$SD = \{e_1 / |e_1| \leq (\lambda_1 \mu h)^{\frac{1}{1-\alpha}}\}. \quad (20)$$

**Remark 3:** The terms  $|e_1|^\alpha$  and  $|e_1|^{2\alpha-1}$  are the explicit parts while the projector (the term  $\mathcal{N}_1$ ) refers to the implicit part. This projector  $\mathcal{N}_1$  cannot be evaluated for  $h = 0$ . Moreover, in (19), to take into account that, at the first time,  $e_1 \in SD$ ,  $E_1$  has no information with respect to  $e_2$  (this will be explained later in (28)). ■

The differentiation error dynamics read as

$$\begin{cases} e_1^+ = e_1 + h(e_2^+ - \lambda_1 \mu |e_1|^\alpha \mathcal{N}_1) \\ e_2^+ = e_2 + h(p^+ - E_1^+ \lambda_2 \mu^2 |e_1|^{2\alpha-1} \mathcal{N}_1) \end{cases} \quad (21)$$

Before presenting the main results, the following assumption is needed.

#### Assumption 2:

- 1) there exists  $\dot{y}_M > 0$  such that for all  $t > 0$ ,  $|\dot{y}(t)| < \dot{y}_M$ ;
- 2) the perturbation  $p(t)$  is a constant parameter or slowly variable, that implies that for sufficient small  $h > 0$ ,  $p^+ \simeq p$ . ■

**Remark 4:** Assumption 2.1 is one of the conditions to stay in  $SD$  (see (26) and after); assumption 2.2 is an extra condition on the perturbation due to the Euler discretization

and the fact that the variation of the perturbation must be negligible over a sampling period. ■

**Theorem 1:** Suppose that Assumptions 1 and 2 hold and  $he_{2M} \in SD$ . Then, for  $h > 0$ , there exist  $\lambda_1 > 0$  and  $\lambda_2 > 0$  such that the differentiation error dynamics (21) converge in finite time to

$$SD_{1,2} = \{e_1, e_2 / e_1 \in SD_1 \text{ and } e_2 \in SD_2\}$$

with

$$\begin{aligned} SD_1 &= \{e_1 / |e_1| \leq \max\{he_{2O1}, he_{2O2}\}\} \\ SD_2 &= \{e_2 / |e_2| \leq \max\{e_{2O1}, e_{2O2}\}\}. \end{aligned}$$

where

$$e_{2O1} = \left| \frac{p_M \lambda_1}{\lambda_2 \mu h^{\alpha-1}} - \frac{\lambda_2 \mu h^\alpha}{\lambda_1} \right| \quad (22)$$

and

$$e_{2O2} = \frac{p_M \lambda_1}{\lambda_2 \mu h^{\alpha-1}} + \frac{\lambda_2 \mu h^\alpha}{2\lambda_1}. \quad (23)$$

*Proof:* The proof is done in three steps: firstly the convergence in finite time of  $e_1$  on  $SD$  is done using the stability analysis of (3). Afterwards, the equilibrium point of  $e_2$  is calculated. Finally, the magnitude of the steady-state oscillations is deduced using the stability analysis of (3).

- Convergence of  $e_1$  in  $(SD)$ . From (19)-(20),  $e_1 \in SD$  if

$$|e_1|^{1-\alpha} < \lambda_1 \mu h \iff |e_1| < (\lambda_1 h \mu)^{\frac{1}{1-\alpha}} \quad (24)$$

the conditions to reach  $SD$  are given in the sequel taking into account that  $e_1 = z + e_{eq}$ . As it is expected at least that for  $z = z_{int}$ , the solution is inside  $SD$ , and (24) reads

$$|z_{int}| + |e_{eq}| < (\lambda_1 h \mu)^{\frac{1}{1-\alpha}} \quad (25)$$

- 1) if  $z$  has the same sign than  $e_2$ , then from (5) including  $a = e_2$  and  $b = \lambda_1 \mu$ , considering (9) and the worth case  $|e_2| = e_{2M}$ , the convergence in  $SD$  in finite time is given by the following inequality

$$\left| \frac{e_{2M}}{\lambda_1 \mu} \right|^{\frac{1}{\alpha}} + \left| \frac{h \lambda_1 \mu}{2} \right|^{\frac{1}{1-\alpha}} < |\lambda_1 \mu h|^{\frac{1}{1-\alpha}} \quad (26)$$

where  $h > 0$  and  $\lambda_1 \mu > 0$  are chosen to satisfy (26). Moreover, to stay in  $SD$ ,  $e_{2M}$  used in (26) must be bounded. This condition is satisfied from assumption 2 and the fact that  $|\hat{x}_2| < \dot{y}_M$  then  $|e_{2M}| < 2\dot{y}_M$ .

- 2) if  $z$  has not the same sign as  $e_2$ , taking the same way than the previous case, considering (10) and the worth case i.e  $|e_2| = e_{2M}$ , it yields

$$|\lambda_1 \mu h|^{\frac{1}{1-\alpha}} > \max \left\{ \left| \frac{e_{2M}}{\lambda_1 \mu} \right|^{\frac{1}{\alpha}} - |h \lambda_1 \mu|^{\frac{1}{1-\alpha}}, \left| \frac{e_{2M}}{\lambda_1 \mu} \right|^{\frac{1}{\alpha}} \right\}. \quad (27)$$

It is always possible to find  $\lambda_1 \mu$  such that (27) is verified.

Remark that for  $e_{2M} = 0$  the oscillation  $z$  is symmetrical around zero and the condition to reach  $SD$  is

$$|\lambda_1 \mu h|^{\frac{1}{1-\alpha}} > \left| \frac{\lambda_1 \mu h}{2} \right|^{\frac{1}{1-\alpha}}$$

that is always verified for  $h, \lambda_1$  and  $\mu$  strictly positive. When  $e_1 \in SD$ , it implies that

$$E_1^+ = 1 \text{ and } \mathcal{N}_1 = \frac{[e_1]^{1-\alpha}}{\lambda_1 h \mu},$$

then  $e_1^+$  verifies the following equation

$$e_1^+ = h e_2^+ \quad (28)$$

and  $e_1$  stays on  $SD$  if  $|e_2^+|$  is smaller than  $e_{2M}$ , which will be proved in the sequel. Then, from (28), on  $SD$ , the second row of (21) becomes

$$e_2^+ = e_2 + h \left( p^+ - \frac{\lambda_2 \mu}{\lambda_1 h} [h e_2]^\alpha \right). \quad (29)$$

**Remark 5:** Equation (29) is the explicit Euler discretization of the following continuous dynamics

$$\dot{e}_2 = p^+ - \frac{\lambda_2 \mu h^{\alpha-1}}{\lambda_1} [e_2]^\alpha \quad (30)$$

and it is well known that explicit Euler discretization of (30) oscillates. ■

• Equilibrium Point of (29). The equilibrium point of (29) is the solution of

$$p^+ - \frac{\lambda_2 \mu}{\lambda_1 h} [h e_2^+]^\alpha = 0. \quad (31)$$

This gives the following equilibrium point  $e_{2,eq}$  for  $e_2$

$$e_{2,eq} = \left( \frac{\lambda_1}{\lambda_2 \mu} p^+ \right)^{\frac{1}{\alpha}} h^{\frac{1-\alpha}{\alpha}}. \quad (32)$$

• Steady-state oscillations of  $e_2$  and  $e_1$ . Remark that (29) is exactly (4) with  $b = \frac{\lambda_2 \mu h^{\alpha-1}}{\lambda_1}$  and  $a = p^+$ . Then setting  $e_2 = z + e_{2,eq}$ , equation (5) is obtained with  $e_{eq} = e_{2,eq}$ . From the previous analysis,  $e_2$  converges in the domain

$$SD2 = \{e_2 / |e_2| \leq \max \{e_{2O1}, e_{2O2}\}\}, \quad (33)$$

where  $e_{2O1}$  and  $e_{2O2}$  are respectively defined in (22)-(23). Remark that the absolute values are removed because all the terms are positive, and  $e_{2M}$  is chosen larger than  $e_{2O1}$  and  $e_{2O2}$ .

Finally, from (28), the oscillation within  $e_1$  is confined inside the  $SD1$  domain

$$SD1 = \{e_1 / |e_1| \leq \max \{h e_{2O1}, h e_{2O2}\}\}. \quad (34)$$

#### IV. SEMI-IMPLICIT HOMOGENEOUS EULER DIFFERENTIATOR WITH TWO PROJECTORS

In order to remove the oscillation on  $e_2$  and consequently on  $e_1$ , the following differentiator with two projectors (SIHD-2) is proposed

$$\begin{cases} \hat{x}_1^+ = \hat{x}_1 + h (\hat{x}_2^+ + \lambda_1 \mu |e_1|^\alpha \mathcal{N}_1) \\ \hat{x}_2^+ = \hat{x}_2 + E_1^+ h (\lambda_2 \mu^2 |e_1|^{2\alpha-1} \mathcal{N}_2) \end{cases} \quad (35)$$

where  $\hat{x}_2^+$  is computed in the first and second rows. The associated projectors are defined by

$$\mathcal{N}_1 := \begin{cases} |e_1|^{1-\alpha} < \lambda_1 \mu h & (e_1^+ = 0) \rightarrow \mathcal{N}_1 = \frac{[e_1]^{1-\alpha}}{\lambda_1 h \mu} \\ |e_1|^{1-\alpha} \geq \lambda_1 \mu h & (e_1^+ \neq 0) \rightarrow \mathcal{N}_1 = \text{sgn}(e_1) \end{cases} \quad (36)$$

and, given that, on  $SD$ ,  $e_1 = h e_2$

$$\mathcal{N}_2 := \begin{cases} |e_1|^{2-2\alpha} < \lambda_2 \mu^2 h^2 \rightarrow \mathcal{N}_2 = \frac{[e_1]^{2-2\alpha}}{\lambda_2 h^2 \mu^2} \\ |e_1|^{2-2\alpha} \geq \lambda_2 \mu^2 h^2 \rightarrow \mathcal{N}_2 = \text{sgn}(e_1) \end{cases} \quad (37)$$

with  $E_1$  defined in (19). The estimation error dynamics read as

$$\begin{cases} e_1^+ = e_1 + h (e_2^+ + \lambda_1 \mu |e_1|^\alpha \mathcal{N}_1) \\ e_2^+ = e_2 + h (p^+ - E_1^+ \lambda_2 \mu^2 |e_1|^{2\alpha-1} \mathcal{N}_2). \end{cases} \quad (38)$$

#### Theorem 2:

Suppose that assumptions 1-2 hold. Then for  $h > 0$ , there exist  $\lambda_1 > 0$  and  $\lambda_2 > 0$  such that the differentiation error dynamics (38) converge in finite time to

$$SD'_{1,2} = \{e_1, e_2 / e_1 \in SD'_1 \text{ and } e_2 \in SD'_2\}$$

with

$$\begin{aligned} SD'1 &= \{e_1 / |e_1| \leq h^2 p_M\}, \\ SD'2 &= \{e_2 / |e_2| \leq h p_M\}. \end{aligned}$$

■

*Proof:* The beginning of the proof is similar to the proof of Theorem 1 concerning the convergence on  $SD$ . After this convergence,  $E_1 = 1$ , and since  $e_1 = h e_2$ , the dynamic of  $e_2^+$  becomes

$$e_2^+ = e_2 + h (p^+ - \lambda_2 \mu^2 h^{2\alpha-1} |e_2|^{2\alpha-1} \mathcal{N}_2).$$

Choosing  $\lambda_2$  sufficiently large after some iterations, it reads  $|e_2|^{2-2\alpha} < \lambda_2 \mu^2 h^{2\alpha}$ . Then, substituting again  $e_1 = h e_2$ , the projector  $\mathcal{N}_2$  can be read as  $\mathcal{N}_2 = \frac{[e_2]^{2-2\alpha}}{\lambda_2 h^{2\alpha} \mu^2}$  and consequently

$$e_2^+ = h p^+$$

■ and finally  $|e_2| \leq h p_M$  and  $|e_1| \leq h^2 p_M$ . ■

## V. $\theta$ PROJECTORS

To improve the robustness with respect to the noise, a modification could be made for the projectors  $\mathcal{N}_1$ , and  $\mathcal{N}_2$  as follows

$$\mathcal{N}_1 := \begin{cases} (1 - \theta)|e_1|^{1-\alpha} < \lambda_1 \mu h & \rightarrow \mathcal{N}_1 = \frac{(1-\theta)|e_1|^{1-\alpha}}{\lambda_1 \mu} \\ (1 - \theta)|e_1|^{1-\alpha} \geq \lambda_1 \mu h & \rightarrow \mathcal{N}_1 = \text{sgn}(e_1) \end{cases}$$

and

$$\mathcal{N}_2 := \begin{cases} |(1 - \theta)e_1|^{2-2\alpha} < \lambda_2 \mu^2 h^2 & \rightarrow \mathcal{N}_2 = \frac{(1-\theta)|e_1|^{2-2\alpha}}{\lambda_2 \mu^2 h^2} \\ |(1 - \theta)e_1|^{2-2\alpha} \geq \lambda_2 \mu^2 h^2 & \rightarrow \mathcal{N}_2 = \text{sgn}(e_1) \end{cases}$$

with  $\theta \in [0, 1)$ . Indeed, to damp the influence of the noise on the sliding surface, instead of requesting  $e_1^+ = 0$ , it is only requested  $e_1^+ = (1 - \theta)e_1$ . From the stability perspective, considering  $\theta$  equal to zero, finite-time convergence is ensured and when  $\theta$  is different from zero, the differentiator is less sensitive to noise, providing only an asymptotic convergence, since the influence of noise on the sliding surface is multiplied by  $(1 - \theta)$ .

## VI. EXPERIMENTAL APPLICATION

In this section, a comparative study illustrates the properties of the proposed versions of the semi-implicit homogeneous differentiation technique. Similarly to the previous work of the authors [14] where some homogeneous differentiation algorithms have been compared in the framework of velocity/acceleration estimation regarding the position of a pneumatic actuator, this study deals with the estimation of the current in the case of an electronics  $RC$  low pass circuit. It aims to compare the performances of the proposed differentiation solutions with a standard first order Butterworth filter<sup>1</sup>. This comparison is mainly based on the analysis of the Sum of Square Error (SSE)<sup>2</sup> applied to the error between each differentiation version and the measured current.

The objective is to differentiate the output of a  $RC$  series circuit ( $R = 100 \Omega$  and  $C = 100 \mu F$ ), this signal being a sine function of frequency  $\omega = 64.71 \text{ rad/s}$  ( $f = 10.3 \text{ Hz}$ ). The measured signal to differentiate - see Fig. 4 has been obtained by scoping the voltage  $v_c$  across the capacitor  $C$ .

Moreover, the voltage  $v_r = R i_c$  is accordingly scoped across the terminals of the resistor  $R$ , and constitutes the reference measured differentiated signal since

$$\dot{v}_c = \frac{1}{RC} v_r. \quad (39)$$

**Remark 6:** By a practical point-of-view, the interest of the differentiator is to avoid the use a current sensor given that  $i_c = C \dot{v}_c$ . ■

<sup>1</sup>The *butter* function of Matlab ® is used to perform a discrete first order high pass filtering.

<sup>2</sup>The SSE is given by  $\text{SSE}(\bullet) = \frac{1}{n} \sum_{l=1}^n \bullet_l^2$  with  $n$  the data size; the second half of the signal (in the steady state) has been considered for the SSE evaluation.

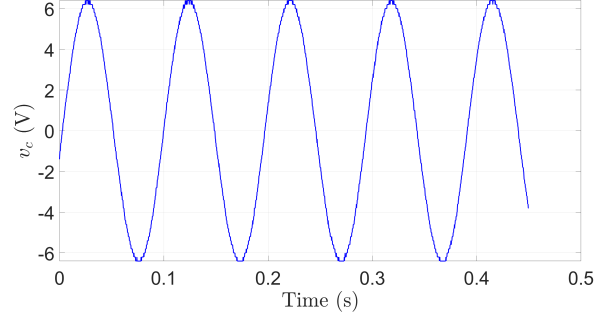


Fig. 4. Measured  $v_c$  versus time (s) for  $h_2 = 2 \cdot 10^{-4}$  s.

Two sampling periods  $h_1 = 2 \cdot 10^{-4}$  s and  $h_2 = 2 \cdot 10^{-3}$  s are considered in the sequel to highlight the properties of the SIHD method at lower sampling.

The Butterworth filter is set at the cutoff frequency of 100 Hz; the parameters of the SIHD methods  $\lambda_1 = \lambda_2 = 10^6$  are chosen to have the linear part stable, and the  $\theta_1$ ,  $\theta_2$ ,  $\alpha$  and  $\mu$  parameters have been obtained thanks to an optimization procedure in order to improve the SSE performance index [15]. These choices are summarized in the following table.

$h$ [s]	method	$\theta_1$	$\theta_2$	$\alpha$	$\mu$	SSE
$2 \cdot 10^{-4}$	Butterw.	-	-	-	-	$2.31 \cdot 10^3$
	SIHD-1	0.95	-	0.64	400	$3.4 \cdot 10^2$
	SIHD-2	0.98	0.37	0.76	0.74	$2.2 \cdot 10^2$
$2 \cdot 10^{-3}$	Butterw.	-	-	-	-	$1.78 \cdot 10^3$
	SIHD-1	0.71	-	0.77	400	$3.9 \cdot 10^2$
	SIHD-2	0.75	0.73	0.65	99.9	$3.7 \cdot 10^2$

Figures 5-6 display the real differentiated signal (obtained from measurement - see (39)) and the outputs of the three differentiators (Butterworth, and the both proposed ones) for the two sampling periods  $h_1$  and  $h_2$ . It appears that, globally, these three solutions allow to get an image of the differentiation, but with a huge difference of performances. Furthermore, the value of the sampling period has an impact on the quality of the differentiation.

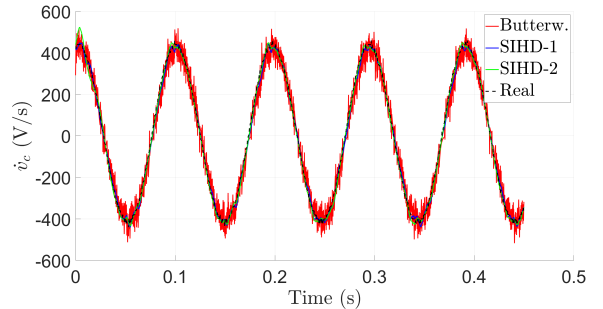


Fig. 5. Differentiated signals (measured, Butterworth, proposed methods) versus time (s) for  $h_1 = 2 \cdot 10^{-4}$  s.

Figures 7 and 8 compare the SSE performances<sup>3</sup> of the

<sup>3</sup>The normalization of SSE in Figures 7 and 8 is made with respect to results obtained with the Butterworth filter (always equal to one).



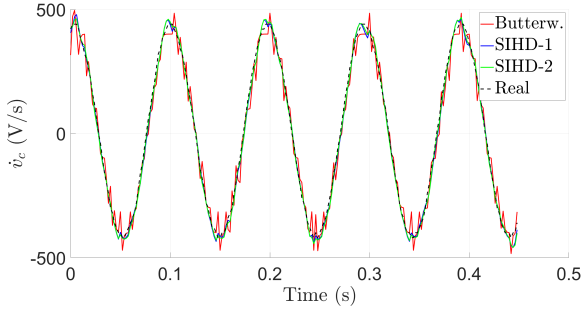


Fig. 6. Differentiated signals (measured, Butterworth, proposed methods) versus time (s) for  $h_2 = 2 \cdot 10^{-3}$ .

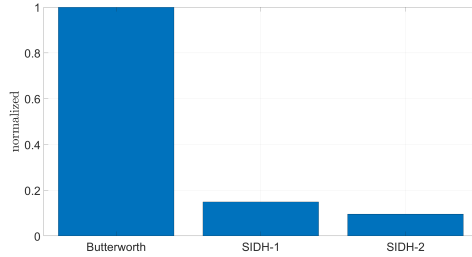


Fig. 7. Evaluation of the normalized index SSE for  $h_1 = 2 \cdot 10^{-4}$  s.

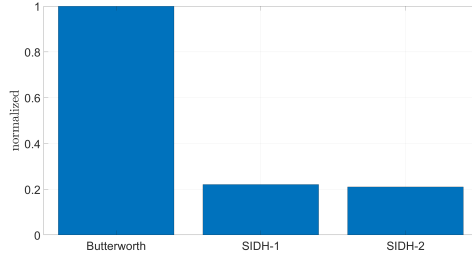


Fig. 8. Evaluation of the normalized index SSE  $h_2 = 2 \cdot 10^{-3}$  s.

SIHD-1 and SIHD-2 according to the Butterworth filter. For both samplings  $h_1$  and  $h_2$ , the semi-implicit homogeneous differentiators show better accuracy regarding the SSE index than the classical Butterworth filter. Since the two-projector-based version (SIHD-2) includes a dedicated projector to drive the tracking error on  $e_2$  and suppress the corresponding oscillations, it provides slightly better performances than the corresponding SIHD-1 method. Moreover, the SIHD-2 method is easier to extend to higher order. Nevertheless in applications, performances and the feasibility of both methods are quite similar (see [14]).

## VII. CONCLUSIONS AND FUTURE WORKS

This paper proposes a semi-implicit Euler approximation of an homogeneous differentiator for a second-order system. The proposed scheme allows to apply an implicit Euler approximation (combined with explicit one) when homogeneous differentiators are considered instead of classical sliding mode differentiators. Two versions of differentiators based on one or two projectors are proposed to reduce

the effect of chattering phenomena, measurement noise and perturbation. These two differentiators and a discrete Butterworth filter (used for comparison) have been implemented and tested on an experimental electronics  $RC$  filter. Better performances have been obtained within the proposed two differentiators compared to the discrete Butterworth filter in term of tracking and noise rejection.

Future investigations include the generalization of the proposed approaches to higher order differentiation as well as extension to variable exponent differentiators to deal with adaptive noise rejection [13]. In addition, more comparisons and investigations will be conducted with respect to recent implicit differentiation techniques. Moreover, it will be very interesting to adapt the Taylor expansion corrective term proposed in [6] to the proposed implicit methods and also to consider not only a regular sampling but also the self and event triggering case [7], [16].

## VIII. ACKNOWLEDGMENTS

This work is supported by *Agence Nationale de la Recherche* (ANR) with project DIGITSLID ANR-18-CE40-0008-01.

## REFERENCES

- [1] M. Spong and M. Vidyasagar, *Robot dynamics and control*. John Wiley, New-York, USA, 1991.
- [2] W. Khalil and E. Dombre, *Modeling, identification and control of robots*. Butterworth Heinemann, 2002.
- [3] M. R. Mojallizadeh and et al., "Discrete-time differentiators in closed-loop control systems: experiments on electropneumatic system and rotary inverted pendulum," [Research Report] INRIA Grenoble. 2021, 2021.
- [4] A. Levant, "Robust exact differentiation via sliding mode technique," *automatica*, vol. 34, no. 3, pp. 379–384, 1998.
- [5] —, "Sliding order and sliding accuracy in sliding mode control," *Int. J. of control*, vol. 58, no. 6, pp. 1247–1263, 1993.
- [6] M. Livne and A. Levant, "Proper discretization of homogeneous differentiators," *Automatica*, vol. 50, no. 8, pp. 2007–2014, 2014.
- [7] J.-P. Barbot, A. Levant, M. Livne, and D. Lunz, "Discrete differentiators based on sliding modes," *Automatica*, vol. 112, p. 108633, 2020.
- [8] V. Acary and B. Brogliato, "Implicit euler numerical scheme and chattering-free implementation of sliding mode systems," *Systems & Control Letters*, vol. 59, no. 5, pp. 284 – 293, 2010.
- [9] A. Polyakov, D. Efimov, and B. Brogliato, "Consistent Discretization of Finite-time and Fixed-time Stable Systems," *SIAM J. on Control and Optimization*, vol. 57, no. 1, pp. 78–103, 2019.
- [10] M. R. Mojallizadeh, B. Brogliato, and V. Acary, "Discrete-time differentiators: design and comparative analysis," hal-02960923v2, 2021.
- [11] J. Jensen, "Sur les fonctions convexes et les inégalités entre les valeurs moyennes," *Acta Math*, vol. 30, pp. 175–193, 1906.
- [12] W. Perruquetti, T. Floquet, and E. Moulay, "Finite-time observers: application to secure communication," *IEEE Trans. on Automatic Control*, vol. 53, no. 1, pp. 356–360, 2008.
- [13] M. Ghanes, J. P. Barbot, L. Fridman, A. Levant, and R. Boisliveau, "A new varying gain exponent based differentiator/observer: an efficient balance between linear and sliding-mode algorithms," *IEEE Trans. on Automatic Control*, 2020.
- [14] L. Michel, S. Selvarajan, M. Ghanes, F. Plestan, Y. Aoustin, and J. P. Barbot, "An experimental investigation of discretized homogeneous differentiators: pneumatic actuator case," *IEEE Journal of Emerging and Selected Topics in Industrial Electronics*, vol. 2, no. 3, pp. 227–236, 2021.
- [15] M. Porcelli and P. L. Toint, "Bfo, a trainable derivative-free brute force optimizer for nonlinear bound-constrained optimization and equilibrium computations with continuous and discrete variables," *ACM Trans. Math. Softw.*, vol. 44, no. 1, Jun. 2017.
- [16] B. Qu, Z. Wang, and B. Shen, "Fusion estimation for a class of multi-rate power systems with randomly occurring scada measurement delays," *Automatica*, vol. 125, p. 109408, 2021.